Descriptor-Guided Mapping of Oxide–Metal Boundary Motifs for Selective C1 Oxygenate Formation

Authors

Ethan J. Miller[1*], Lauren E. Parker[2]

Affiliations

Department of Chemical Engineering, Massachusetts Institute of Technology, 25 Ames Street, Cambridge, MA 02139, USA

***Corresponding author:** ethanmiller@mit.edu

Abstract

The catalytic formation of C1 oxygenates depends strongly on the local geometry and electronic structure of oxide–metal boundary motifs, yet the structural diversity of these interfacial sites makes rational catalyst design difficult. In this work, a descriptor-guided computational framework was developed to identify active boundary motifs for selective C1 oxygenate formation over oxide-decorated copper surfaces. A dataset containing 124 oxide–Cu interfacial configurations was constructed by varying oxide nuclearity, metal–oxygen coordination, interfacial oxygen vacancy density, and exposed Cu facet. Density functional theory calculations were performed to obtain adsorption energies of CO_2*, HCOO*, H_2COO*, CH_3O*, CO*, and H_2O*, together with 214 transition-state barriers along methanol and CO formation pathways. The results show that the adsorption energy difference between HCOO* and CO* is a reliable selectivity descriptor, with a Pearson correlation coefficient of 0.81 for methanol selectivity predicted by microkinetic modeling. Motifs with partially reduced ZrOx and TiOx clusters on stepped Cu surfaces showed the most favorable balance between CO_2 activation and intermediate hydrogenation, reducing the HCOO* hydrogenation barrier by 0.28–0.44 eV compared with flat Cu(111). A gradient-boosting regression model trained on geometric and electronic descriptors predicted methanol formation barriers with a mean absolute error of 0.067 eV. Microkinetic simulations at 240 °C and 30 bar further indicated that boundary motifs with moderate oxophilicity could increase the methanol-to-CO rate ratio by more than one order of magnitude. This study provides a transferable descriptor framework for screening oxide–metal catalytic ensembles and highlights the importance of interfacial site diversity in controlling C1 oxygenate selectivity.

Keywords: oxide–metal interface; C1 oxygenates; catalyst descriptor; density functional theory; microkinetic modeling; machine learning; interfacial ensemble

1. Introduction

CO_2 hydrogenation to methanol provides a promising route for carbon utilization and renewable-energy storage by converting CO_2 and green H_2 into a transportable liquid product.

Methanol is widely used as a fuel, hydrogen carrier, solvent, and chemical feedstock and can also serve as an intermediate for the production of olefins, hydrocarbons, and other value-added chemicals. Cu-based catalysts remain among the most extensively investigated systems for methanol synthesis because Cu efficiently activates H_2 and enables hydrogenation reactions under comparatively moderate temperatures and pressures. Nevertheless, the catalytic behavior of practical Cu-based materials cannot be explained by metallic Cu alone. Increasing evidence indicates that methanol formation is strongly associated with oxide–Cu interfacial regions, where oxide-derived sites facilitate the adsorption and stabilization of CO_2-derived intermediates while neighboring Cu atoms provide activated hydrogen [1,2]. Oxides such as ZrO_x, ZnO_x, TiO_x, and CeO_x can modify the local electronic structure of Cu, generate coordinatively unsaturated sites or oxygen vacancies, and alter the adsorption strengths of key C_1 intermediates. These interfacial effects are particularly important because CO_2 hydrogenation involves competition between methanol synthesis and CO formation through the reverse water–gas shift pathway. Excessively weak adsorption may limit CO_2 activation, whereas overly strong adsorption can stabilize formate, methoxy, CO, or oxygen-containing species and slow their subsequent conversion or removal. An effective interface must therefore provide a suitable balance between CO_2 activation, hydrogen transfer, intermediate stabilization, and product desorption rather than simply maximizing adsorption strength [3,4].

The atomic structure of the oxide–Cu boundary is consequently a major factor controlling activity and selectivity. Recent ensemble-based calculations on inverse ZrO_2/Cu catalysts have shown that catalytic performance cannot necessarily be represented by a single optimized active-site geometry. A broad set of interfacial configurations accessible under reaction conditions displayed markedly different reactivities, and only a limited subset remained highly active throughout the complete methanol formation pathway [5]. The analysis further showed that states formed after methoxy production can strongly influence the overall turnover rate and that structural evolution of the interface may shift the catalyst population from more active toward less active configurations, establishing a direct connection between interfacial flexibility, reactivity, and deactivation [6,7]. This observation is important because oxide clusters supported on Cu are unlikely to remain as one rigid idealized structure during reaction. Their coordination environment can change with adsorbate coverage, hydrogenation state, vacancy formation, and interaction with the underlying metal. Related studies have also demonstrated pronounced structure sensitivity in other Cu–oxide systems. Isolated Cu–O units associated with ZrO_2 can favor methanol formation, whereas local structures containing stronger Cu–Cu interactions may promote CO production [8,9]. Changes in oxide dispersion, interfacial coordination, and metal oxidation state have similarly been associated with altered methanol selectivity in Cu/TiO_2, Cu–In_2O_3, CuZn–CeO_x, and CuZn/$ZnZrO_x$ catalysts [10,11]. Taken together, these results suggest that nominal catalyst composition or total Cu surface area alone is insufficient to describe catalytic performance. The detailed geometry, coordination, and electronic environment of individual oxide–Cu boundary

motifs must also be considered. Density functional theory (DFT) has provided substantial insight into these structure–reactivity relationships by resolving elementary steps that are difficult to distinguish experimentally. Proposed pathways for CO_2 hydrogenation include formate, carboxyl, dioxymethylene, formaldehyde, methoxy, and CO-derived intermediates, and their relative importance varies with oxide identity, Cu facet, oxygen-vacancy concentration, hydrogen coverage, and local coordination. Calculations on oxide clusters supported on TiO_2, for example, have demonstrated that different interfacial sites may separately control CO_2 adsorption, H_2 activation, and subsequent hydrogenation steps [12,13]. Studies of Cu/ZnO and chemically modified Cu surfaces have likewise related changes in coordination and charge distribution to the activation barriers governing methanol and CO formation [14,15]. Such results emphasize that adsorption thermodynamics alone does not completely determine catalytic performance. A structure that binds a desired intermediate favorably may still exhibit a large kinetic barrier for its hydrogenation, while another structure with apparently less favorable adsorption may provide a lower-energy transition state and a higher turnover rate. Surface coverage introduces an additional complication because adsorbate–adsorbate interactions and competitive adsorption of H_2O, CO, and oxygen-containing intermediates can alter both reaction energies and accessible active-site configurations under realistic conditions. Despite this progress, most atomistic studies examine only a small number of manually selected surfaces or interface geometries. Idealized Cu facets decorated with one oxide cluster size, one vacancy configuration, or one metal–oxygen coordination environment are often used as representative models. Such an approach is suitable for clarifying individual reaction mechanisms but provides only limited information about the broader structural diversity of oxide–Cu catalysts. It also makes systematic comparison difficult because oxide size, oxygen coordination, vacancy density, exposed Cu facet, and interfacial geometry are frequently changed independently across different studies. The resulting calculations therefore offer detailed mechanistic information for specific structures but do not readily reveal transferable structural rules for identifying active motifs. The ensemble behavior reported for inverse ZrO_2/Cu further strengthens this concern by showing that even chemically similar interface configurations can exhibit substantially different catalytic behavior [16]. A broader structural dataset is needed to determine whether common geometric or electronic characteristics can distinguish active methanol-forming interfaces from structures that favor CO formation or become kinetically trapped by strongly adsorbed intermediates. Descriptor-based modeling and machine-learning approaches provide a practical route for addressing this structural complexity. Previous models have incorporated catalyst composition, reaction conditions, adsorption energies, atomic charges, coordination numbers, and other physicochemical variables to predict methanol activity or identify promising catalyst compositions [17,18]. These approaches can reduce the computational cost of exploring large materials spaces and can reveal nonlinear relationships that are difficult to identify from individual DFT calculations. However, many existing models are constructed from bulk catalyst properties or experimentally measured performance and therefore

do not explicitly resolve individual oxide–Cu boundary sites. Models based primarily on adsorption energies face an additional limitation because adsorption descriptors represent thermodynamic stability rather than the kinetic accessibility of the full reaction sequence. Similar adsorption energies may correspond to substantially different transition-state barriers, and a descriptor correlated with CO_2 activation may not necessarily distinguish methanol formation from competing CO production. Reliable screening of interfacial active motifs therefore requires closer integration of structural descriptors, adsorption thermodynamics, elementary-reaction barriers, and reaction kinetics. Microkinetic analysis is particularly useful in this context because it translates elementary energetics into predicted turnover rates and selectivities under specified reaction conditions and can test whether a proposed descriptor remains meaningful after coverage and kinetic competition are considered.

In this work, a descriptor-based computational framework is developed to systematically map active motifs on oxide-decorated Cu surfaces and to establish quantitative relationships between interfacial structure, elementary reaction energetics, and methanol selectivity. A dataset containing 124 oxide–Cu interface structures is constructed to cover variations in oxide cluster size, metal–oxygen coordination number, oxygen-vacancy density, and exposed Cu surface geometry, including both flat and stepped Cu facets. Adsorption energies are calculated for CO_2*, HCOO*, H_2COO*, CH_3O*, CO*, and H_2O*, providing a consistent description of the principal adsorbed states involved in methanol synthesis and competing CO formation. To move beyond adsorption-energy screening, 214 transition-state barriers are further determined for elementary steps along the relevant methanol and CO pathways. Geometric and electronic characteristics of the interface are then used as input features for a gradient-boosting regression model to determine which local structural variables most strongly govern adsorption and activation energetics. The predicted relationships are subsequently evaluated through microkinetic simulations at 240 °C and 30 bar so that candidate descriptors can be tested against reaction rates and product selectivity rather than adsorption thermodynamics alone. Particular attention is given to the energy difference between HCOO* and CO* as a potential selectivity descriptor, because these intermediates represent competing tendencies toward oxygenate retention and CO formation. ZrO_x, TiO_x, and other oxide motifs are compared across different Cu environments to determine how oxide chemistry and surface geometry jointly regulate CO_2 binding, intermediate hydrogenation, and CO release. By combining systematic interface sampling, transition-state calculations, machine-learning analysis, and microkinetic validation within a common dataset, this study aims to bridge the gap between detailed mechanistic calculations on individual structures and efficient screening of structurally diverse oxide–Cu interfaces. The resulting framework is intended to identify physically interpretable boundary motifs that achieve balanced CO_2 activation, rapid hydrogenation of methanol-forming intermediates, and suppression of competing CO formation, thereby providing atomistic design principles for more active and selective Cu-based methanol synthesis catalysts.

2. Materials and Methods

2.1 Model Dataset and Structural Space

A dataset of 124 oxide–Cu boundary structures was prepared to cover different interfacial sites. The models included ZrO_x, TiO_x, CeO_x, ZnO_x, and MgO_x clusters on Cu(111), Cu(100), Cu(211), and Cu(221) surfaces. Each oxide cluster contained one to six metal atoms. The structures differed in cluster size, metal–oxygen coordination, oxygen-vacancy content, and Cu coordination. Each slab contained four Cu layers. The bottom two layers were fixed during optimization. A vacuum space of 16 Å was added along the surface-normal direction. The dataset included flat and stepped Cu surfaces, stoichiometric oxide clusters, partly reduced clusters, and vacancy-rich interfaces.

2.2 Computational Design and Control Models

The 124 structures were grouped by oxide type, Cu surface, oxide reduction state, and boundary shape. Bare Cu surfaces were used as control models. Stoichiometric oxide clusters were compared with reduced clusters to examine the effect of oxygen vacancies. Flat Cu(111) surfaces were compared with stepped Cu surfaces to test the role of low-coordination Cu atoms. Other control models had similar oxide sizes but different metal–oxygen coordination. These models were used to separate the effect of local structure from that of oxide composition. Methanol and CO formation routes were studied on all suitable models. The main steps included CO_2 activation, formate formation, formate hydrogenation, dioxymethylene formation, methoxy formation, CO production, water release, and methanol desorption.

2.3 DFT Calculations and Quality Control

Spin-polarized density functional theory calculations were carried out with the projector-augmented-wave method and the PBE functional. The D3 correction was used for dispersion forces. The plane-wave cutoff was set to 500 eV. A $3\times3\times1$ Monkhorst–Pack grid was used for the main cells. Electronic energies were converged to 10^{-5} eV. Atomic positions were optimized until the force on each free atom was below 0.02 eV $Å^{-1}$. Transition states were located with the climbing-image nudged elastic band method. Each transition state was checked by frequency analysis and had one imaginary frequency along the reaction path. Key adsorption energies and reaction barriers were recalculated with a denser kkk-point grid. Energy changes below 0.03 eV were accepted as converged. Duplicate structures were removed by comparing bond lengths and coordination numbers.

2.4 Descriptor Processing and Model Equations

Adsorption energies were calculated from the energies of the adsorbed system, clean surface, and gas-phase molecule:

$$E_{ads} = E_{surface+adsorbate} - E_{surface} - E_{gas}$$

The selectivity descriptor was defined as the adsorption-energy difference between HCOO* and CO*:

$$\Delta E_{sel} = E_{ads}(HCOO^*) - E_{ads}(CO^*)$$

The geometric descriptors included Cu coordination number, oxide cluster size, metal–oxygen coordination, vacancy density, interfacial bond length, and Cu step density. The electronic descriptors included Bader charge, d-band center, work function, and local magnetic moment. All variables were standardized before model training. Features with correlation coefficients above 0.95 were reduced to limit repeated information. Pearson correlation analysis was used to compare each descriptor with methanol selectivity and reaction barriers.

2.5 Machine-Learning and Microkinetic Analysis

Gradient-boosting regression was used to predict methanol formation barriers from the geometric and electronic descriptors. The dataset was divided into training, validation, and test sets at a ratio of 70:15:15. Five-fold cross-validation was used to tune the model settings. Model accuracy was measured by mean absolute error, root mean square error, and the coefficient of determination. Microkinetic simulations were carried out at 240 °C and 30 bar with an H_2/CO_2 molar ratio of 3. The kinetic model included adsorption, desorption, hydrogenation, reverse water–gas shift, methanol formation, CO formation, and water removal. Steady-state surface coverages were obtained by solving the coupled rate equations until all coverage changes were below 10^{-10} s^{-1}. Sensitivity tests were performed for temperature, pressure, oxide type, and vacancy density. Models that failed site or elemental balance were removed from the final analysis.

3. Results and Discussion

3.1 Descriptor Mapping of Oxide–Cu Boundary Sites

The 124 interface models showed large differences in adsorption behavior. Oxide type alone did not explain these differences. Oxide size, vacancy content, Cu coordination, and metal–oxygen bonding also affected the binding of C_1 species. The adsorption-energy difference between HCOO* and CO* showed the strongest link with methanol selectivity, with a Pearson correlation coefficient of 0.81. Sites that stabilized HCOO* relative to CO* generally favored methanol formation. Strong CO* binding promoted the reverse water–gas shift route. However, overly strong HCOO* binding slowed later hydrogenation steps. The best sites therefore showed moderate HCOO* binding rather than the strongest adsorption. Partly reduced ZrO_x and TiO_x clusters on stepped Cu surfaces fell within this range, as shown in Fig. 1. Liang et al. (2026) also found that small ZrO_2 domains on Cu formed active boundary sites for CO_2 hydrogenation. Shaik et al. (2025) reported that small metal groups near oxide defects improved formate hydrogenation. The present study extends these findings by comparing several oxide types under the same calculation method [19,20].

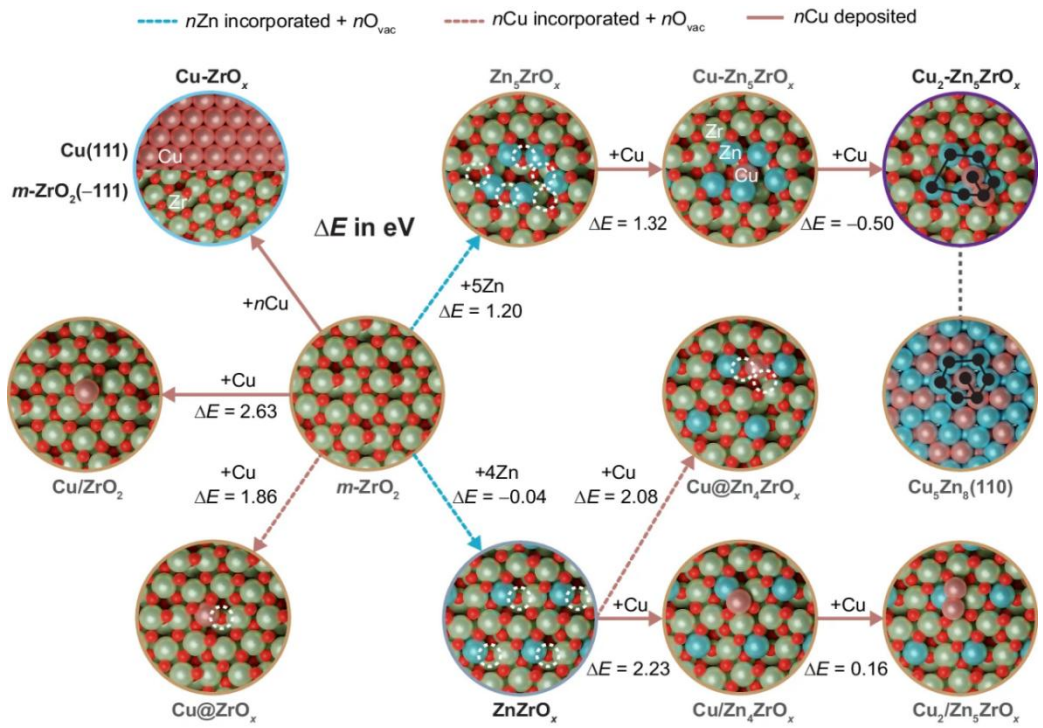

Fig. 1. Oxide–Cu boundary sites, adsorption-energy differences, and HCOO* hydrogenation barriers.

3.2 Reaction Barriers on Flat and Stepped Cu Surfaces

Stepped Cu surfaces showed lower reaction barriers than flat Cu(111) when suitable oxide clusters were present. Low-coordination Cu atoms improved H_2 splitting, while nearby oxide sites stabilized oxygen-containing intermediates. Partly reduced ZrO_x and TiO_x sites lowered the HCOO* hydrogenation barrier by 0.28–0.44 eV relative to Cu(111). This decrease came from the shorter distance between Cu-bound H and the oxygen atoms of HCOO*. The oxide clusters also stabilized H_2COO* without binding CH_3O* too strongly. In contrast, vacancy-free clusters showed weak CO_2 activation. Highly reduced clusters bound some intermediates too strongly. MgO_x sites favored carbonate-like species but showed high barriers for later hydrogenation. ZnO_x and CeO_x sites gave middle-range behavior that depended on local coordination. Yang et (2026) also showed that direct Cu–ZrO_2 contact was needed for selective methanol formation. The present results further show that the shape and reduction state of this contact control the reaction barrier [21].

3.3 Prediction of Methanol Formation Barriers

The gradient-boosting model predicted the DFT barriers with a mean absolute error of 0.067 eV. This error was smaller than the barrier differences among the main groups of boundary sites. The model could therefore separate less active structures from ZrO_x–Cu and TiO_x–Cu sites with lower barriers. Both geometric and electronic features were needed for accurate prediction. Models based only on oxide type or Cu surface gave lower accuracy because structures with the

same composition often had different coordination and charge. The agreement between the DFT and predicted barriers is shown in Fig. 2. Wu et al. (2026) used machine learning to predict methanol yield from catalyst composition and reaction conditions. The present model works at the atomic scale and predicts elementary reaction barriers from local site features. It can therefore reduce the number of costly transition-state calculations during catalyst screening.

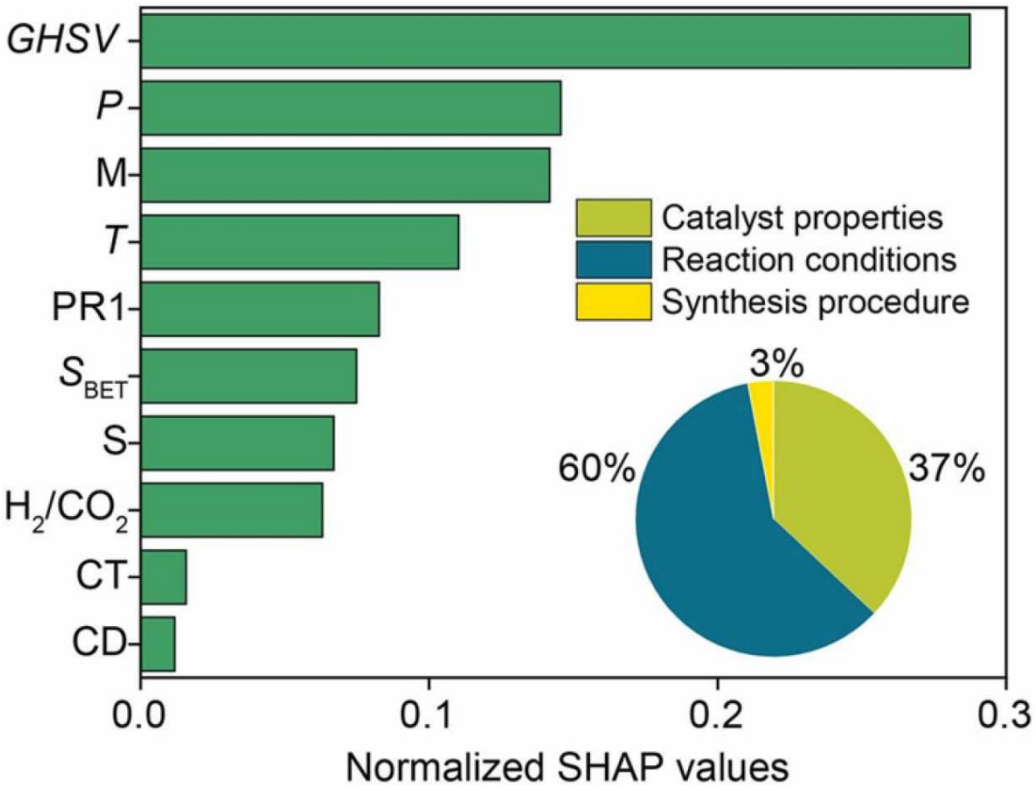

Fig. 2. Predicted reaction barriers and methanol selectivity at oxide–Cu boundary sites.

3.4 Microkinetic Selectivity and Catalyst Design

Microkinetic simulations at 240 °C and 30 bar showed that the descriptor map could separate methanol-forming sites from CO-forming sites. Boundary sites with moderate oxygen affinity increased the methanol-to-CO rate ratio by more than ten times compared with Cu(111). These sites adsorbed CO_2 strongly enough to form HCOO* but did not trap HCOO*, H_2COO*, or CH_3O*. Sites with very strong oxygen affinity accumulated stable oxygen-containing species and slowed product release. Weak sites gave low HCOO* coverage and allowed CO formation to compete. The best performance came from low-coordination Cu atoms next to partly reduced ZrO_x or TiO_x clusters. These sites combined H_2 splitting on Cu with CO_2 activation and C_1 hydrogenation at the boundary. This result agrees with earlier studies showing that methanol formation requires close contact between Cu and oxide sites [22,23]. It also explains why oxide loading alone cannot predict activity. A small oxide cluster with suitable coordination can be more active than a larger cluster with poor boundary structure. The HCOO*–CO* adsorption-energy difference can therefore be used for early screening, while machine-learning and microkinetic models can be used for later checks.

4. Conclusion

Analysis of 124 oxide–Cu boundary structures identified the site features that control C1 oxygenate selectivity. The adsorption-energy difference between HCOO* and CO* was closely related to methanol selectivity, with a Pearson correlation coefficient of 0.81. Partly reduced ZrO_x and TiO_x clusters on stepped Cu surfaces gave the best balance between CO_2 adsorption and intermediate hydrogenation. These sites lowered the HCOO* hydrogenation barrier by 0.28–0.44 eV compared with Cu(111). The gradient-boosting model predicted methanol formation barriers with a mean absolute error of 0.067 eV. This accuracy shows that local geometric and electronic features can be used to screen active boundary sites. Microkinetic simulations at 240 °C and 30 bar showed that sites with moderate oxygen affinity increased the methanol-to-CO rate ratio by more than tenfold. The results link boundary structure with adsorption strength, reaction barriers, and product selectivity. This method may help screen oxide–metal sites for methanol synthesis and other C1 conversion reactions. However, the calculations used fixed surface structures and a limited group of oxides. Further work should examine surface changes during reaction, higher intermediate coverage, larger oxide clusters, and experimental tests of the predicted sites.

References

1. Asif, M., Bilal, M., Hakeem, L., Asghar, G., Manzoor, S., Hira, ... & Khan, S. A. (2026). Catalytic Confinement Engineering for CO2 Conversion: From Catalytic Microenvironments to Sustainable Aviation Fuels. Carbon Neutralization, 5(4), e70186.

2. Gu, X. (2026). Identifying Causal Effects and Analyzing Heterogeneity of User Growth Interventions on Digital Platforms: Evidence from Large-Scale Behavioral Data. Available at SSRN 6809181.

3. You, S. (2026). Verifiable Audit Mechanisms in AI Compliance Automation: Scalability. Available at SSRN 6547458.

4. Pasvei, S., Hosseini Moradi, S. A., & Namvar, F. (2026). Recent advances in activated carbons for CO2 capture: Structure–performance relationships and future perspectives. Adsorption Science & Technology, 44, 02636174251414478.

5. Yang, Z., Alexandrova, A. N., & Sautet, P. (2026). Modeling CO2 Hydrogenation to Methanol on an Ensemble of Inverse ZrO2 on Cu Catalytic Sites: Mechanism, Reactivity, and Deactivation. Angewandte Chemie, e5448247.

6. Jiao, Y., Shi, T., Zhao, B., & Wang, A. (2026). The Impact of VR Sketching Simulations on the Assessment of Scale and Site Suitability in Public Art Spaces.

7. Berroug, N., Gutiérrez-Ortiz, M. A., González-Velasco, J. R., & Boukha, Z. (2026). Effect of Ni Particle Size on the Efficiency of Ni/HAP Grafted Catalysts in the CO2 Methanation Reaction. ChemCatChem, 18(15), e71004.

8. Bao, Y., Qiu, Y., & Wang, H. (2026, May). Unified Identity Layer for Hyperscale Ecosystems: A Framework for Cross-Platform User Attribution and Experimentation. In 2026 6th International Conference on Machine Learning and Intelligent Systems Engineering (MLISE) (pp. 540-543). IEEE.
9. Jurado Apolo, D. A. (2025). Theoretical studies investigating the mechanism of methanol formation over Cu/ZnO based catalysts (Doctoral dissertation, Albert-Ludwigs-Universität Freiburg).
10. Chen, F., Liang, H., Li, S., Yue, L., & Xu, P. (2025). Design of Domestic Chip Scheduling Architecture for Smart Grid Based on Edge Collaboration.
11. Liang, R., Feifan, F. N. U., Liang, Y., & Ye, Z. (2025). Emotion-Aware Interface Adaptation in Mobile Applications Based on Color Psychology and Multimodal User State Recognition. Frontiers in Artificial Intelligence Research, 2(1), 51-57.
12. Sebastian, J., Mebrahtu, C., Zeng, F., & Palkovits, R. (2026). Strong Metal-Support Interactions on TiO2-Supported Metal Catalysts for Fine-Tuning Catalysis. Angewandte Chemie International Edition, 65(1), e02611.
13. Du, Y. (2025). Research on Digital Quality Traceability System for Temperature-Controlled Supply Chain of Foreign Trade Wine Driven by Blockchain and IoT. Business and Social Sciences Proceedings, 4, 57-65.
14. Jurado Apolo, D. A. (2025). Theoretical studies investigating the mechanism of methanol formation over Cu/ZnO based catalysts (Doctoral dissertation, Albert-Ludwigs-Universität Freiburg).
15. Liang, S., Zhang, X., Du, Y., & Chen, W. (2026). Supply Network Restructuring and Capacity Ramp-Up Limits in the Localized Expansion of High-Performance Computing Equipment Production. Available at SSRN 7339738.
16. Harrison, J. A., Smith, E. R., & Davies, A. P. (2026). Interfacial Site Ensembles Drive Methanol Selectivity on ZrO2-on-Cu Inverse Catalysts. Global Media and Social Sciences Research Journal, 7(1), 175-180.
17. Bao, Y., & Wang, H. (2026). Edge-to-Cloud Infrastructure Continuum: A Unified Framework for Optimizing Industrial IoT Systems. Available at SSRN 7185578.
18. Tsipoaka, M., & Rownaghi, A. A. (2025). Toward Understanding the Stability of Single-Atom Catalysts in Oxygen Evolution Reactions. Advanced Energy Materials, 15(29), 2500635.
19. Jiao, Y., Zhao, B., Wang, A., & Shi, T. (2026). Construction and Empirical Study of a Modularized Teaching System for Art Courses Based on a Unified Training Pathway.
20. Shaik, S. A., Nigam, P. K., & Gugulothu, S. K. (2025). Advanced fin designs for improved thermal management in PCM-based latent heat storage systems. Applied Thermal Engineering, 272, 126337.
21. Yang, J. (2026). Stage-Coupled Computational Framework for Stratified Accessibility and Equity Analysis in Community-Based Elderly Care Services.

22. Comas-Vives, A., & Copéret, C. (2026). Nature and dynamics of active sites in Cu-based catalysts for the CO2 hydrogenation to methanol. Accounts of Chemical Research, 59(1), 27-39.
23. Wu, J., Wu, D., Zhang, J., & Peng, Y. (2026). Generative AI Feedback in Junior High School Artistic Creation Evaluation. Available at SSRN 7244838.